Indian J Phys (February 2014) 88(2):119–127
DOI 10.1007/s12648-013-0398-x

ORIGINAL PAPER

Theoretical study of molecular structures, vibrational and NMR spectra on azobenzene derivatives

M Karakaya* and F Ucun

Department of Physics, Faculty of Arts and Sciences, Süleyman Demirel University, 32260 Isparta, Turkey

Received: 05 June 2013 / Accepted: 29 August 2013 / Published online: 26 September 2013

Abstract: In this study, we have calculated the most stable tautomeric forms and their ground state conformers of 2,4-dihydroxyazobenzene and 2,4-dihydroxy-6-methyl-4′-nitroazobenzene molecules. Calculations show that the most preferential tautomeric forms of these molecules are azo form for 2,4-dihydroxyazobenzene and hydrazo form for 2,4-dihydroxy-6-methyl-4′-nitroazobenzene. Vibrational frequencies, ^{1}H and ^{13}C NMR shifts of ground state conformers of stable tautomeric forms of the molecules have been calculated by using density functional theory-B3LYP method with 6-311G(d,p) basis set. All assignments of theoretical frequencies have been performed by potential energy distribution analysis. Calculated spectral results are in a good agreement with the corresponding experimental data.

Keywords: 2,4-Dihydroxyazobenzene; 2,4-Dihydroxy-6-methyl-4′-nitroazobenzene; IR spectra; NMR spectra; Density functional theory

PACS No.: 31.15.-p

1. Introduction

Azobenzene derivatives are of great potential in developing optical materials such as data storage devices [1–5]. They improve remarkable isomerization properties [6] with two stable conformers (*trans* and *cis*) easily accessible through appropriate photon absorption. Besides mechanism for thermal *cis–trans* isomerization of azobenzenes has been studied extensively and the effect of substituents, solvent polarity and pressure has been discussed [7]. The combined studies of NMR and electronic spectroscopies have been recently carried out on tautomeric structures of azobenzene derivatives [8].

Tautomeric forms of disazo dyes have different colors, tinctorial strengths (and hence economics) and different properties, e.g. light fastness. Some authors have investigated tautomeric structure of barbituric acid dyes in the solid state using FT-IR [9]. It has been found that disazo dyes exist in tri-keto forms in solid state while they are in azo-enol forms in solvents [10].

In present study, the most stable tautomeric forms of 2,4-dihydroxyazobenzene and 2,4-dihydroxy-6-methyl-4′-nitroazobenzene molecules have been obtained and then, vibrational frequencies, ^{1}H and ^{13}C NMR shift values of their designed most stable conformers have been calculated and compared with experimental data. Recently, similar studies for various materials have been reported by density functional theory and other methods [11, 12].

2. Computational details

All computations were done by using Gaussian 03 package [13] and Gauss-View molecular visualization programs [14] on personal computer. Vibrational frequencies of 2,4-dihydroxyazobenzene (azo-1) and 2,4-dihydroxy-6-methyl-4′-nitroazobenzene (azo-2) molecules were calculated by density functional theory-B3LYP (DFT/B3LYP) method at 6-311G(d,p) basis set level. The calculated vibration frequencies were scaled with a scale factor of 0.9614 [15] and clarified and assigned by means of potential energy distribution (PED) analysis using VEDA 4 program [16]. ^{1}H and ^{13}C NMR chemical shifts (in DMSO solvent) were done by Gauge Including

*Corresponding author, E-mail: mkarakayafizik@hotmail.com

Atomic Orbitals (GIAO) method and the solvent effects were taken into account by means of PCM approximation using the same set level of theory, routinely used for NMR chemical shift calculations on fairly large molecules [17, 18]. In chemical shift calculations, tetramethylsilane (TMS) was used as a reference molecule and the theoretical chemical shift ^{1}H and ^{13}C values were obtained by subtracting GIAO isotropic magnetic shielding (IMS) values [19, 20]. To find the optimum transition states of these molecules, quantum synchronous transit2 (QST2) approaches were used by taking their optimized azo and hydrazo forms.

3. Results and discussion

3.1. Ground state conformer analysis and tautomeric forms

Firstly, in order to find the most stable conformers of azo-1 and azo-2 molecules, detailed potential energy surface (PES) scans in dihedral angles 13C–12C–22N–21N and 13C–11C–20N–19N have been performed, respectively. The scans are done by minimizing the potential energy by changing these dihedral angles every 20° for 360° rotation (from −180° to 180° in 18 steps) around the bond. All of PES scans are performed by DFT/B3LYP method at 6-31G (d) basis set level. Graphs of PES scans of the title compounds are given in Figs. 1 and 2.

Minimum energy structures after scanning are optimized by DFT (B3LYP) method at 6-311G (d,p) basis set. These structures with atom numberings are also situated in Figs. 3 and 4. Molecular weights of azo-1 ($C_{12}H_{10}N_2O_2$) and azo-2 ($C_{13}H_{11}N_3O_4$) are 214.22 and 273.2 g mol^{-1}, respectively. Melting point range for azo-1 compound is given as 143–146 °C in literature [21, 22].

Then, potential energy surface (PES) scans have been done by changing the bond length 23O–24H form 0.9 to 1.8 Å in steps of 0.05 Å using DFT/B3LYP method at 6--31G(d) basis set level. These results are given in Figs. 5 and 6. As seen from these figures, azo form for azo-1 molecule and hydrazo form for azo-2 molecule are more stable. The relative and barrier energy values between azo and hydrazo forms are 0.11, 4.14 kcal/mol for the azo-1 and 0.96, 4.37 kcal/mol for azo-2, respectively.

3.2. Vibrational frequencies, symmetries and assignments

Resulting vibrational frequencies for the lowest energy conformers of title compounds are given in Tables 1 and 2. For comparison, experimental vibrational frequencies (IR) of the molecules are given in tables [21]. As also realized

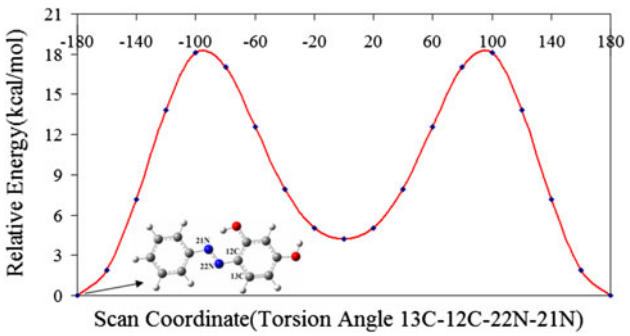

Fig. 1 Potential energy surface scan graph of azo-1

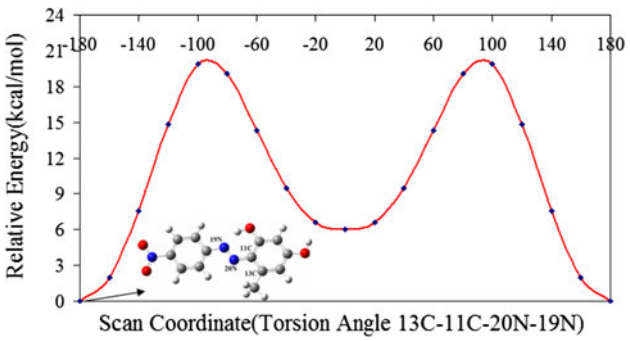

Fig. 2 Potential energy surface scan graph of azo-2

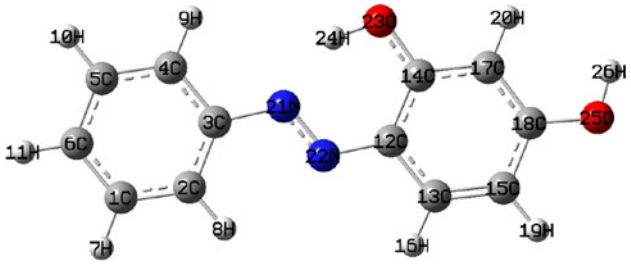

Fig. 3 Optimized molecular structure of azo-1

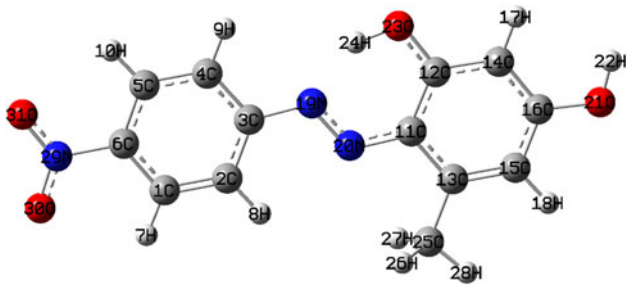

Fig. 4 Optimized molecular structure of azo-2

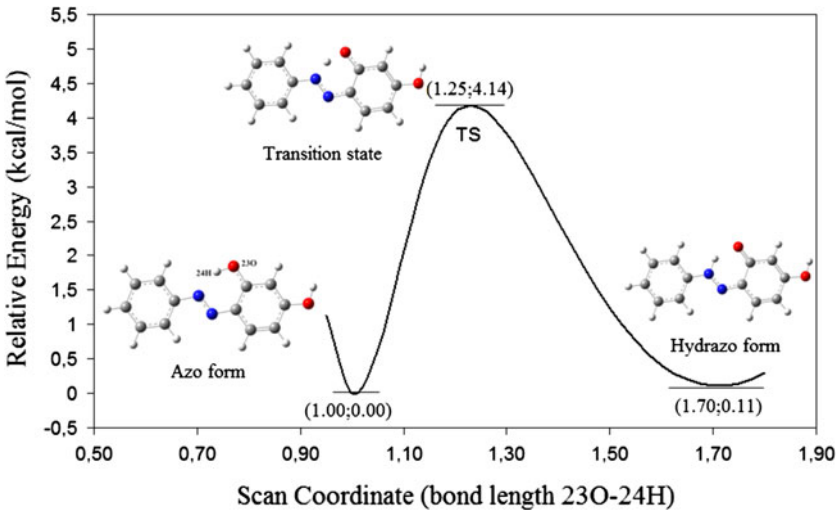

Fig. 5 Potential energy surface scan graph of azo-1 for azo and hydrazo form

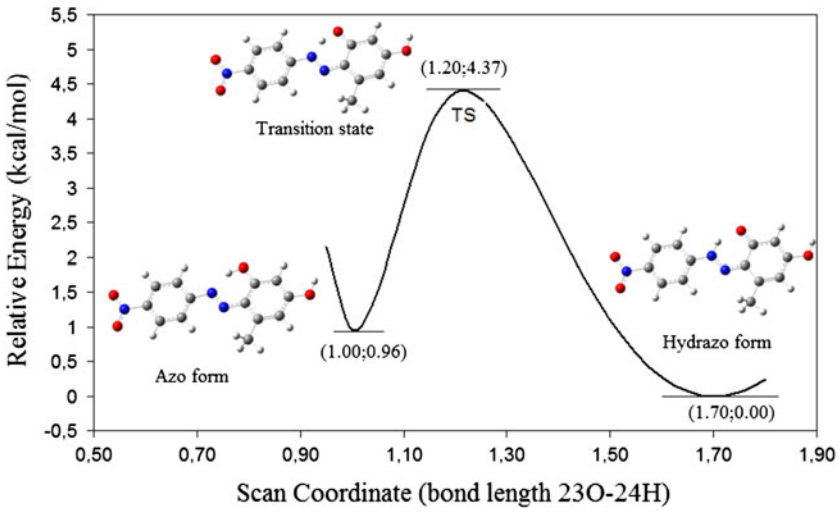

Fig. 6 Potential energy surface scan graph of azo-2 for azo and hydrazo form

from Figs. 3, 4, the molecules are planar and belong to C_s point group. So, vibrations being symmetric through the mirror plane σ_h belongs to species A' and the ones being anti-symmetric to species A''. Numbers of vibration modes is $\Gamma_{vib.} = 49A' + 23A''$ for azo-1 and $\Gamma_{vib.} = 59A' + 28A''$ for the azo-2, respectively. Symmetry species of all vibrational modes are given in Tables 1 and 2. Assignments of all fundamental vibrational modes obtained by using VEDA 4 programs are also given in Tables 1 and 2. The frequency values are computed at range of 3,043–3,089 cm^{-1} for azo-1 and 3,054–3,103 cm^{-1} for azo-2 with highest % PED for C–H (aromatic) stretching. Also, the values of frequencies of azo-1 and azo-2 for N=N stretching mode have been calculated as 1,476 and 1,470 cm^{-1}, respectively. In an earlier study, experimental frequencies value of azobenzene, a similar molecule, for N=N stretching mode is observed at 1,511 cm^{-1} band by Zimmermann et al. [23]. Correlation values (R^2), root mean square errors (RMSE) and mean absolute error (MAE) between experimental and calculated frequencies are shown in last rows of Tables 1 and 2. They show a good agreement with each other.

3.3. Chemical shifts

Calculated ^1H and ^{13}C NMR chemical shifts (with respect to TMS) for ground state conformers of the title compounds are displayed in Tables 3 and 4. Values of experimental chemical shift for azo-1 in Table 3 have been obtained from spectral database for organic compounds web page [21]. But those for azo-2 is not found in the literature. Correlation factors between experimental and theoretical chemical shifts are shown in last rows of Table 3. According to these values, it can be stated that the agreement between experimental and calculated chemical shifts is good.

Table 1 Experimental and calculated vibrational frequencies, their symmeries and assignments of azo-1

Mode no.	Symmetry	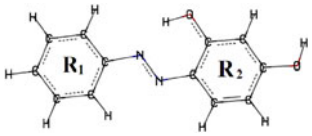	Experimental IR frequencies (cm^{-1})[b]	Calculated frequencies (cm^{-1}) DFT/B3LYP method 6-311G(d,p) basis set	
			Azo-1	Unscaled	Scaled
		Assignments and % PED[a]			
72	A′	ν_{OH}(100)(4-hydroxy)		3,823	3,675
71	A′	$R_1[\nu_{CH}(99)$ sym]	3077sh	3,213	3,089
70	A′	$R_2[\nu_{CH}(100)$ sym]		3,209	3,085
69	A′	$R_1[\nu_{CH}(94)$ sym]		3,193	3,070
68	A′	$R_2[\nu_{CH}(95)$ asym]		3,191	3,068
67	A′	$R_1[\nu_{CH}(93)$ asym]		3,184	3,061
66	A′	$R_1[\nu_{CH}(93)$ asym]	2954vs	3,174	3,051
65	A′	$R_2[\nu_{CH}(99)$ asym]	2924vs	3,170	3,048
64	A′	$R_1[\nu_{CH}(99)$ asym]	2855vs	3,165	3,043
63	A′	ν_{OH}(98)(2-hydroxy)		3,133	3,012
62	A′	$(R_1 + R_2)[\nu_{CC}$ (26)]	1627m	1,672	1,608
61	A′	$(R_1 + R_2)[\nu_{CC}$ (57)] + $R_1[\delta_{HCC}(19)]$	1590m	1,640	1,576
60	A′	$R_2[\nu_{CC}(26)] + \delta_{HOC}(17) + (R_1 + R_2)[\delta_{CCC}(11)]$		1,630	1,567
59	A′	$(R_1 + R_2)[\nu_{CC}$ (37) + $\delta_{CCC}(20)]$	1528m	1,623	1,560
58	A′	$\delta_{HOC}(23) + R_2[\nu_{CC}(21) + \delta_{HCC}(21)]$	1489m	1,553	1,493
57	A′	$\nu_{NN}(29)$	1467s	1,535	1,476
56	A′	$R_1[\delta_{HCC}(56) + \delta_{CCC}(10)]$	1458s	1,512	1,454
55	A′	$(R_1 + R_2)[\delta_{HCC}(40) + \nu_{CC}(12)]$		1,490	1,433
54	A′	$\delta_{HOC}(29) + \nu_{NN}(12)$	1411sh	1,463	1,407
53	A′	$\nu_{NN}(40)$	1378m	1,441	1,385
52	A′	$(R_1 + R_2)[\nu_{CC}(20)] + \nu_{OC}(16) + \delta_{HOC}(13)$	1357m	1,366	1,313
51	A′	$\nu_{OC}(17) + (R_1 + R_2)[\nu_{CC}(17)] + R_2[\delta_{HCC}(10) + \delta_{CCC}(10)]$	1308m	1,358	1,306
50	A′	$(R_1 + R_2)[\nu_{CC}(35) + \delta_{HCC}(28)]$		1,348	1,296
49	A′	$R_1[\delta_{HCC}(50)] + (R_1 + R_2)[\nu_{CC}(12)]$		1,337	1,286
48	A′	$(R_1 + R_2)[\nu_{CN}(47)] + R_2[\delta_{HCC}(10)]$	1252br	1,285	1,235
47	A′	$\delta_{HOC}(12) + (R_1 + R_2)[\delta_{HCC}(10)]$	1192sh	1,255	1,206
46	A′	$\nu_{CC}(33) + R_2[\delta_{HCC}(12)] + (R_1 + R_2)[\nu_{NC}(10)]$		1,224	1,176
45	A′	$(R_1 + R_2)[\nu_{NC}(20)] + \nu_{OC}(14)$		1,220	1,173
44	A′	$\delta_{HOC}(36) + R_2[\delta_{HCC}(22)]$	1157m	1,193	1,146
43	A′	$R_1[\delta_{HCC}(71)] + (R_1 + R_2)[\nu_{CC}(14)]$		1,181	1,135
42	A′	$R_1[\delta_{HCC}(53)] + (R_1 + R_2)[\nu_{NC}(10)]$	1118m	1,177	1,131
41	A′	$R_2[\delta_{HCC}(61)]$	1108m	1,134	1,090
40	A′	$R_1[\delta_{HCC}(28) + \nu_{CC}(14)]$	1072m	1,101	1,058
39	A′	$R_1[\nu_{CC}(48) + \delta_{HCC}(25) + \delta_{CCC}(10)]$		1,042	1,001
38	A′	$R_1[\delta_{CCC}(58) + \nu_{CC}(20)]$	979m	1,015	976
37	A″	$R_1[\tau_{HCCC}(63)]$		1,010	971
36	A′	$R_2[\delta_{CCC}(16) + \nu_{CC}(14)] + \nu_{OC}(11)$		991	953
35	A″	$R_1[\tau_{HCCC}(70) + \tau_{CCCC}(13)]$		990	952
34	A″	$R_2[\tau_{HCCC}(82)]$		965	928
33	A″	$R_1[\tau_{HCCC}(81) + \gamma_{NCCC}(10)]$		945	908
32	A′	$R_2[\delta_{CNN}(20)] + R_1[\delta_{NNC}(19)] + (R_1 + R_2)[\delta_{CCC}(10)]$		938	902

Table 1 continued

Mode no.	Symmetry	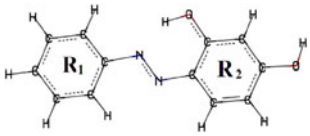	Experimental IR frequencies (cm^{-1})[b]	Calculated frequencies (cm^{-1}) DFT/B3LYP method 6-311G(d,p) basis set	
			Azo-1	Unscaled	Scaled
		Assignments and % PED[a]			
31	A″	$\tau_{HOCC}(83)$	858w	885	851
30	A″	$R_1[\tau_{HCCC}(96)]$	822m	854	821
29	A′	$(R_1 + R_2)[\nu_{NC}(22)] + R_2[\delta_{CCC}(10)]$	808m	828	796
28	A″	$R_2[\tau_{HCCC}(39)]$		825	793
27	A″	$R_2[\tau_{HCCC}(63)] + \gamma_{OCCC}(10)]$		821	789
26	A″	$R_1[\tau_{HCCC}(51) + \gamma_{NCCC}(19)]$	769m	788	757
25	A′	$(R_1 + R_2)[\delta_{CCC}(42)] + R_2[\nu_{OC}(14) + \nu_{CC}(14)]$	723m	758	728
24	A″	$R_2[\tau_{CCCC}(22) + \gamma_{OCCC}(20) + \tau_{HCCC}(15)]$	683m	725	697
23	A″	$R_1[\tau_{CCCC}(49) + \tau_{HCCC}(27)] + R_2[\tau_{HCCC}(10)]$	664m	703	675
22	A″	$\gamma_{OCCC}(55) + R_2[\tau_{HCCC}(20)]$		658	632
21	A′	$(R_1 + R_2)[\delta_{CCC}(43)]$	626m	657	631
20	A′	$R_1[\delta_{CCC}(56)]$	607w	633	608
19	A′	$R_2[\delta_{CCC}(26) + \delta_{CCN}(21)] + \delta_{OCC}(14)$		611	588
18	A″	$R_1[\gamma_{NCCC}(27) + \tau_{HCCC}(12)] + \tau_{CNNC}(16) + (R_1 + R_2)[\tau_{CCCC}(11)]$	522m	540	520
17	A′	$(R_1 + R_2)[\delta_{CCC}(36)] + \delta_{OCC}(13) + \nu_{OC}(11)$		528	508
16	A′	$(R_1 + R_2)[\delta_{CCC}(26)] + R_1[\delta_{NCC}(11)]$	486br	501	482
15	A′	$\delta_{OCC}(46) + R_2[\delta_{CCC}(10)]$		474	456
14	A″	$R_2[\tau_{CCCC}(39)] + \gamma_{OCCC}(20)$		468	450
13	A″	$R_1[\tau_{CCCC}(74)]$		419	402
12	A″	$\tau_{HOCC}(41) + (R_1 + R_2)[\tau_{CCCC}(20)] + \gamma_{OCCC}(12)$		412	396
11	A″	$\tau_{HOCC}(65)$		402	386
10	A′	$\delta_{OCC}(72)$		360	346
09	A″	$R_1[\tau_{CCCC}(36) + \tau_{NNCC}(10)] + R_2[\tau_{CCNN}(24)]$		310	298
08	A′	$R_2[\delta_{CCN}(28)] + R_1[\delta_{NCC}(25)]$		278	268
07	A″	$R_2[\tau_{CCCC}(42)] + \gamma_{OCCC}(19)$		233	224
06	A′	$(R_1 + R_2)[\nu_{NC}(21) + \delta_{CCC}(20)] + R_1[\delta_{NCC}(10)] + R_2[\delta_{CNN}(10)]$		220	212
05	A″	$(R_1 + R_2)[\tau_{CCCC}(55)] + R_2[\tau_{CCNN}(21)]$		217	209
04	A″	$(R_1 + R_2)[\tau_{CCCC}(51)] + R_1[\gamma_{NCCC}(15 + R_2[\tau_{CCNN}(12)]$		121	117
03	A′	$R_1[\delta_{NNC}(36) + \delta_{NCC}(17)] + R_2[\delta_{CNN}(27) + \delta_{CCN}(14)]$		81	78
02	A″	$\tau_{CNNC}(36) + (R_1 + R_2)[\tau_{CCCC}(30)] + (R_1)[\gamma_{NCCC}(12)]$		48	46
01	A″	$R_1[\tau_{NNCC}(76)] + R_2[\tau_{CCNN}(12)]$		26	25
			R^2	0.9980501	0.9980504
			RMSE	93.51	45.41
			MAE	64.00	22.63

[a] Potential energy distribution (PED) of 2,4-dihydroxyazobenzene, less than 10 % are not shown

[b] Taken from Ref. [21]

v stretching, *δ* bending, *γ* out of plane bending, *τ* torsion modes, *sym* symmetric, *asym* anti symmetric, *w* weak, *m* medium, *s* strong, *v* very, *sh* shoulder, *br* broad

Table 2 Experimental and calculated vibrational frequencies, their symmeries and assignments of azo-2

Mode no.	Symmetry	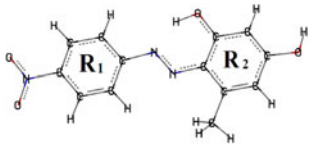	Experimental IR frequencies (cm^{-1})[b]	Calculated frequencies (cm^{-1}) DFT/B3LYP method 6-311G(d,p) basis set	
			Azo-2	Unscaled	Scaled
		Assignments and % PED[a]			
87	A′	ν_{OH}(100)(4-hydroxy)		3,818	3,671
86	A′	$R_1[\nu_{CH}(96)$ sym]		3,228	3,103
85	A′	$R_1[\nu_{CH}(100)$ asym]		3,227	3,102
84	A′	$R_1[\nu_{CH}(98)$ asym]		3,216	3,092
83	A′	$R_2[\nu_{CH}(100)]$		3,198	3,074
82	A′	$R_1[\nu_{CH}(99)$ asym]		3,192	3,069
81	A′	$R_2[\nu_{CH}(100)]$		3,177	3,054
80	A′	$Me[\nu_{CH}(97)$ asym]		3,119	2,998
79	A′	$Me[\nu_{CH}(100)$ asym]	2966vs	3,098	2,978
78	A′	ν_{OH}(97)(2-hydroxy)	2925vs	3,063	2,945
77	A′	$Me[\nu_{CH}(97)$ sym]	2855s	3,043	2,926
76	A′	$(R_1 + R_2)[\nu_{CC}(51)] + \delta_{HOC}(12)$	1625m	1,674	1,609
75	A′	$R_1[\nu_{CC}(39) + \nu_{ON}(27)]$	1606m	1,647	1,584
74	A′	$R_1[\nu_{CC}(52)]$	1595sh	1,635	1,572
73	A′	$R_2[\nu_{CC}(31) + \delta_{HOC}(21) + \delta_{CCC}(12)]$		1,622	1,560
72	A′	$R_1[\nu_{ON}(61) + \nu_{CC}(17)]$		1,590	1,529
71	A′	$R_2[\nu_{CC}(25) + \delta_{HOC}(20)]$	1508s	1,555	1,495
70	A′	$Me[\delta_{HCH}(14)] + \nu_{NN}(12) + \delta_{HOC}(10)$	1467s	1,529	1,470
69	A′	$R_1[\delta_{HCC}(55) + \nu_{CC}(12) + \delta_{CCC}(11)]$		1,512	1,454
68	A′	$Me[\delta_{HCH}(47) + \tau_{HCCC}(16)]$		1,493	1,435
67	A″	$Me[\delta_{HCH}(80) + \tau_{HCCC}(19)]$		1,480	1,423
66	A′	$\nu_{NN}(25) + (R_1 + R_2)[\nu_{CC}(10)]$		1,461	1,404
65	A′	$R_2[\nu_{CC}(20) + \nu_{OC}(20)] + Me[\delta_{HCH}(10)]$		1,448	1,392
64	A′	$\nu_{NN}(29)$	1378m	1,434	1,379
63	A′	$Me[\delta_{HCH}(91)]$		1,418	1,364
62	A′	$R_1[\nu_{ON}(39)]$	1338s	1,376	1,323
61	A′	$R_1[\nu_{ON}(28)] + (R_1 + R_2)[\nu_{CC}(36)]$		1,373	1,320
60	A′	$(R_1 + R_2)[\nu_{CC}(43)]$		1,359	1,307
59	A′	$\nu_{OC}(12) + \nu_{NN}(10)$		1,333	1,281
58	A′	$R_1[\delta_{HCC}(70)]$		1,317	1,266
57	A′	$(R_1 + R_2)[\nu_{NC}(42)]$		1,297	1,247
56	A′	$R_2[\delta_{HOC}(25)] + R_2[\delta_{HCC}(22)]$	1223m	1,257	1,209
55	A′	$(R_1 + R_2)[\nu_{NC}(29)] + \nu_{OC}(12) + R_1[\delta_{HCC}(70)]$		1,230	1,183
54	A′	$\nu_{OC}(40) + R_2[\delta_{HCC}(34)]$	1165m	1,203	1,157
53	A′	$R_2[\delta_{HOC}(37)] + R_2[\delta_{HCC}(31)]$	1145m	1,195	1,149
52	A′	$R_1[\delta_{HCC}(42)]$	1107m	1,178	1,133
51	A′	$R_1[\delta_{HCC}(71)]$		1,123	1,079
50	A′	$R_1[\nu_{CC}(32) + (\nu_{NC}(19) + (\delta_{HCC}(10)]$		1,118	1,075
49	A′	$Me[\tau_{HCCC}(21)] + R_2[\nu_{CC}(14)]$		1,087	1,045
48	A″	$Me[\tau_{HCCC}(55)] + Me[\delta_{HCH}(19)] + R_2[\gamma_{CCCC}(10)]$	1027sh	1,061	1,020
47	A′	$(R_1 + R_2)[\delta_{CCC}(52)]$		1,021	982
46	A′	$R_2[\nu_{CC}(23)] + Me[\tau_{HCCC}(14)]$	973m	1,017	977
45	A″	$R_1[\tau_{HCCC}(73)]$		1,009	970
44	A′	$Me[\tau_{HCCC}(26)]$		1,001	962
43	A″	$R_1[\tau_{HCCC}(77) + \tau_{CCCC}(13)]$		993	955
42	A′	$R_1[\delta_{CCC}(17) + \delta_{NNC}(15) + \delta_{CNN}(12) + \nu_{CC}(11)]$		933	897
41	A″	$R_2[\tau_{HOCC}(74)]$	866sh	907	872

Table 2 continued

Mode no.	Symmetry	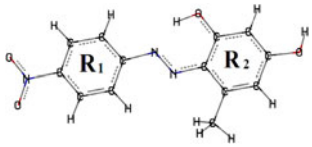	Experimental IR frequencies (cm^{-1})[b]	Calculated frequencies (cm^{-1}) DFT/B3LYP method 6-311G(d,p) basis set	
			Azo-2	Unscaled	Scaled
		Assignments and % PED[a]			
40	A″	$R_1[\tau_{HCCC}(64) + \gamma_{NCCC}(11)]$	851s	884	850
39	A′	$R_1[\delta_{ONO}(44) + \nu_{CC}(13) + \nu_{ON}(12)]$		873	839
38	A″	$R_2[\tau_{HCCC}(67) + \gamma_{OCCC}(10)]$		850	817
37	A″	$R_1[\tau_{HCCC}(97)]$		847	814
36	A′	$\nu_{NC}(16) + (R_1 + R_2)[\delta_{CCC}(11)] + R_1[\delta_{ONO}(10)]$	802sh	825	794
35	A″	$R_2[\tau_{HCCC}(63) + \gamma_{OCCC}(24)]$		817	785
34	A″	$R_1[\gamma_{OCON}(35) + \gamma_{NCCC}(34)]$	749m	759	730
33	A″	$R_2[\gamma_{CCCC}(20) + \gamma_{OCON}(17) + \gamma_{OCCC}(10)]$		741	713
32	A″	$R_1[\gamma_{OCON}(34) + \tau_{HCCC}(27)]$	687w	704	677
31	A′	$R_1[\delta_{CCC}(27) + \delta_{ONO}(15) + \nu_{NC}(10)]$		697	670
30	A″	$R_2[\gamma_{OCCC}(52) + \tau_{HCCC}(23)]$		663	637
29	A′	$R_1[\delta_{CCC}(23) + \delta_{NCC}(12) + \nu_{CC}(10)] + R_2[\delta_{CCN}(10)]$		650	625
28	A′	$R_2[\delta_{OCC}(24) + \delta_{CCN}(17)] + (R_1 + R_2)[\delta_{CCC}(11)]$		627	603
27	A′	$R_2[\nu_{CC}(46) + \nu_{OC}(21)]$		596	573
26	A″	$R_2[\gamma_{CCCC}(29) + \gamma_{OCCC}(23)]$		569	547
25	A′	$R_1[\delta_{ONC}(22)] + (R_1 + R_2)[\delta_{CCC}(18)]$		550	529
24	A′	$R_1[\delta_{ONC}(30)] + (R_1 + R_2)[\delta_{CCC}(10)]$		531	510
23	A″	$R_1[\gamma_{NCCC}(38) + \tau_{CCCC}(23) + \tau_{CNNC}(13)]$		524	504
22	A′	$R_2[\delta_{CCC}(48) + \delta_{OCC}(20)]$	497br	520	500
21	A′	$(R_1 + R_2)[\delta_{CCC}(17)] + R_1[\delta_{NCC}(13) + \delta_{ONC}(12)] + R_2[\delta_{CNN}(12) + \delta_{OCC}(10)]$		485	466
20	A″	$R_2[\tau_{HOCC}(90)]$		431	415
19	A″	$R_1[\tau_{CCCC}(46) + \tau_{HCCC}(10)]$		424	408
18	A″	$R_2[\tau_{CCCN}(23) + \gamma_{OCCC}(11)] + \tau_{CNNC}(11)]$		411	396
17	A′	$(R_1 + R_2)[\delta_{CCC}(27)] + R_1[\nu_{NC}(46))]$		409	393
16	A′	$R_2[\delta_{OCC}(52)]$		369	355
15	A″	$R_1[\tau_{CCCC}(23) + \gamma_{NCCC}(18)] + R_2[\tau_{CCNN}(14)]$		342	329
14	A′	$R_2[\delta_{OCC}(37) + \delta_{CCC}(25)]$		323	311
13	A′	$R_1[\delta_{NCC}(28) + \delta_{ONC}(13)] + R_2[\delta_{CCC}(20) + \delta_{CCN}(13)]$		286	275
12	A″	$R_2[\tau_{CCNN}(40)] + R_1[\tau_{CCCC}(14) + \tau_{NCCC}(11)]$		252	242
11	A″	$R_2[\tau_{CCCC}(72)]$		226	217
10	A′	$R_1[\delta_{NCC}(16) + \delta_{CCC}(10)] + (R_1 + R_2)[\nu_{NC}(12)] + R_2[\delta_{CCN}(10)]$		198	191
09	A″	$R_1[\gamma_{OCCC}(20) + \gamma_{CCCC}(18) + \tau_{CCCC}(14)]$		197	190
08	A′	$R_1[\delta_{HCC}(43) + \delta_{NCC}(30) + \nu_{NC}(12)] + R_2[\delta_{CNN}(15) + \delta_{CCN}(11)]$		178	171
07	A″	$\tau_{CNNC}(17)] + R_1[\gamma_{NCCC}(13)] + (R_1 + R_2)[\tau_{CCCC}(11)]$		163	157
06	A″	$Me[\tau_{HCCC}(71)] + R_2[\gamma_{CCCC}(20)]$		136	131
05	A″	$(R_1 + R_2)[\tau_{CCCC}(55)]$		80	77
04	A″	$R_1[\delta_{NNC}(37) + \delta_{NCC}(20)]$		59	57
03	A′	$R_2[\delta_{CNN}(24)]$		58	56
02	A″	$\tau_{CNNC}(26) + (R_1 + R_2)[\tau_{CCCC}(27)] + R_1[\gamma_{NCCC}(10)]$		32	31
01	A″	$R_1[\tau_{NNCC}(59)] + \tau_{CNNC}(13)$		19	18
			R^2	0.999389	0.999387
			RMSE	69.27	13.91
			MAE	54.95	20.05

[a] Potential energy distribution (PED) of 2,4-dihydroxy-6-methyl-4′-nitroazobenzene, less than 10 % are not shown

[b] Taken from Ref. [21]

v stretching, *δ* bending, *γ* out of plane bending, *τ* torsion modes, *sym* symmetric, *asym* anti symmetric, *Me* methyl, *w* weak, *m* medium, *s* strong, *v* very, *sh* shoulder, *br* broad

Table 3 Experimental and calculated chemical shift values (with respect to TMS) for lowest-energy conformer of azo-1 with GIAO method

Atoms	Experimental (ppm)[a]	Calculated B3LYP/6-311G(d,p) basis set GIAO method	
	Azo-1	Azo-1	
	(solvent: DMSO)	(solvent: DMSO)	(solvent: none)
1-C	129.29	135.25	134.49
2-C	121.51	118.47	119.23
3-C	150.52	157.29	157.64
4-C	121.51	135.45	135.27
5-C	129.29	135.66	134.52
6-C	130.18	137.05	135.55
12-C	132.19	138.62	138.95
13-C	129.29	143.50	143.77
14-C	156.28	164.49	165.22
15-C	109.05	113.11	112.10
17-C	102.92	105.83	104.87
18-C	162.93	170.99	169.33
	R^2	0.9504	0.9502
	RMSE	8.0275	7.7342
	MAE	7.2358	6.7117
7-H	7.55	7.92	7.58
8-H	7.86	8.37	8.26
9-H	7.86	8.12	7.84
10-H	7.55	8.02	7.65
11-H	7.48	7.88	7.50
16-H	7.70	8.16	7.90
19-H	6.52	6.99	6.70
20-H	6.38	6.67	6.13
24-H	10.60	13.57	13.64
	R^2	0.9641	0.9662
	RMSE	1.0637	1.0300
	MAE	0.6889	0.4711

[a] Taken from Ref. [21]

Table 4 Calculated chemical shift values (with respect to TMS) for lowest-energy conformer of azo-2 with GIAO method

Atoms	Calculated B3LYP/6-311G(d.p) basis set GIAO method Azo-2 (solvent: none)
1-C	130.50
2-C	118.68
3-C	161.56
4-C	133.47
5-C	130.88
6-C	155.07
11-C	138.84
12-C	166.67
13-C	155.28
14-C	103.47
15-C	115.21
16-C	171.43
25-C	22.63
7-H	8.49
8-H	8.20
9-H	7.79
10-H	8.57
17-H	6.01
18-H	6.61
22-H	4.38
24-H	14.34
26-H(methyl)	2.93
27-H(methyl)	2.93
28-H(methyl)	2.03

4. Conclusions

In present study, the most stable tautomeric forms and their ground state conformers of 2,4-dihydroxyazobenzene and 2,4-dihydroxy-6-methyl-4′-nitroazobenzene molecules were investigated. The most stable tautomeric forms were found as azo form for azo-1 and hydrazo form for azo-2. Also, the theoretical vibrational frequencies and ^{1}H and ^{13}C NMR shift values of ground state conformers of these molecules were obtained by using density functional theory (DFT/B3LYP) method with 6-311G(d,p) basis set. All the assignments of theoretical frequencies were done by potential energy distribution (PED) analysis. Generally, it could be said that calculated results of the molecules were in a good agreement with experimental data. Some incompatibility of calculations with the experimental data can be attributed that molecular geometries in vapour phase may be different from that in the solid phase, owing to extended hydrogen bonding and stacking interactions.

References

[1] H Zollinger *Color Chemistry: Synthesis, Properties and Applications of Organic Dyes and Pigments* (Weinheim: WILEY-VCH) p 186 (1991)
[2] J L Humphrey, K M Lott, M E Wright and D Kuciauskas *J. Phys. Chem.* **B109** 21496 (2005)
[3] S K Yesodha, C K S Pillai and N Tsutsumi *Prog. Polym. Sci.* **29** 45 (2004)
[4] J -L Zhou, X -F Chen, X -H Fan, C -X Lu and Q -F Zhou *J. Polym. Sci. A Polym. Chem.* **44** 6047 (2006)
[5] N Li, J Lu, Q Xu and L Wang *Opt. Mater.* **28** 141 (2006)
[6] K Ichimura *Chem. Rev.* **100** 1847 (2000)
[7] M Azuki, K Morihashi, T Watanabe, O Takahashi and O Kikuchi *J. Mol. Struc. (Theochem)* **542** 255 (2001)
[8] P L Tarifa, G S Sanz, I Alkorta, J Elguero, D Sanz, A Perona and R M Claramunt *J. Mol. Struc.* **1015** 138 (2012)
[9] R Gup, E Giziroglu and B Kırkan *Dyes Pigments* **73** 40 (2007)

[10] F Karci and F Karci *Dyes Pigments* **77** 451 (2008)
[11] Y Sert, F Ucun and M Böyükata *Indian J. Phys.* **87** 113 (2013)
[12] T Rasheed and S Ahmad *Indian J. Phys.* **85** 239 (2011)
[13] M J Frisch et al. *Gaussian 03: Revision C.02* (Pittsburgh: Gaussian Inc.) (2003)
[14] A Frisch, A B Nielsen and A J Holder *Gauss View User Manual* (Pittsburgh: Gaussian Inc.) (2001)
[15] D C Young *Computional Chemistry: A Pratical Guide for Applying Techniques to Real-World Problems* (New York: Wiley) (2001)
[16] M H Jamroz *Vibrational Energy Distribution Analysis VEDA 4* (Warsaw) (2004)
[17] J Cheeseman, G Trucks, T Keith and M Frisch *J. Chem. Phys.* **104** 5497 (1996)
[18] T A Keith and R F W Bader *Chem. Phys. Lett.* **210** 223 (1993)
[19] R Ditchfield *Mol. Phys.* **27** 789 (1974)
[20] C M Rohlfing, L C Allen and R Ditchfield *Chem. Phys.* **87** 9 (1984)
[21] http://riodb01.ibase.aist.go.jp/sdbs/cgi-bin/cre_index.cgi?lang=eng (last accessed on Feb. 2013)
[22] http://www.sigmaaldrich.com/european-export.html (last accessed on Feb. 2013)
[23] F Zimmermann, T H Lippert, C H Beyer, J Stebani, O Nuyken and A Wokaun *Appl. Spectrosc.* **47** 7 (1993)